

# Evolution of Dust-to-Metal Ratio in Galaxies

Akio K. INOUE<sup>\*†</sup>

*Department of Astronomy, Kyoto University, Sakyo-ku, Kyoto 606-8502  
 inoue@kusastro.kyoto-u.ac.jp*

(Received 2003 March 31; accepted 2003 June 28)

## Abstract

This paper investigates the evolution of the dust-to-metal ratio in galaxies based on a simple evolution model for the amount of metal and dust with infall. We take into account grain formation in stellar mass-loss gas, grain growth by the accretion of metallic atoms in a cold dense cloud, and grain destruction by SNe shocks. Especially, we propose that the accretion efficiency is independent of the star-formation history. This predicts various evolutionary tracks in the metallicity ( $Z$ )–dust-to-gas ratio ( $\mathcal{D}$ ) plane depending on the star-formation history. In this framework, the observed linear  $Z$ – $\mathcal{D}$  relation of nearby spiral galaxies can be interpreted as a sequence of a constant galactic age. We emphasize that an observational study of the  $Z$ – $\mathcal{D}$  relation of galaxies at  $z \sim 1$  is very useful to constrain the efficiencies of dust growth and destruction. We also suggest that the Lyman break galaxies at  $z \sim 3$  have a very low dust-to-metal ratio, typically  $\lesssim 0.1$ . Although the effect of infall on the evolutionary tracks in the  $Z$ – $\mathcal{D}$  plane is quite small, the dispersion of the infall rate can disturb the  $Z$ – $\mathcal{D}$  relation with a constant galactic age.

**Key words:** dust, extinction — galaxies: evolution — galaxies: ISM — ISM: evolution

## 1. Introduction

Because dust exists everywhere, stellar light is dimmed by the interstellar dust, strong far-infrared radiation from dust is observed, and the interstellar gas is heated/cooled by some processes involving dust. Moreover, comets and planets are made from dust, and various molecules are formed on dust. Therefore, dust is one of the most important constituents of galaxies and the universe (e.g., Whittet 2003).

In the context of research on the galaxy evolution, knowledge of the dust amount in galaxies is essential to extract the physical properties of galaxies from observations. This is because radiation from stars is always extinguished to some extent by internal dust attenuation. Since it is difficult to estimate the precise amount of attenuation from the observed photometric data (e.g., Buat, et al. 2002), any other information about the amount of dust is very useful. One may think that the metallicity is a good tracer of the amount of dust. This is true if the dust-to-metal ratio can be regarded as universal.

Dust grains are made from metal elements, which are injected into the interstellar medium (ISM) by stellar mass-loss at the end of, or during, stellar evolution. The evolution of the amount of metal in a galaxy is traced as a consequence of the star formation activity of the galaxy. To date, such metallicity evolution has been studied very well since classical work in the 1970s (e.g., Audouze, Tinsley 1976; Tinsley 1980 for reviews). The evolution of the amount of dust can be traced by an extension of the evolution of metal-

licity if we take account of the formation, destruction, and growth processes of dust grains in the ISM. After the pioneering work by Dwek, Scalo (1980), some authors have examined this subject (Wang 1991; Lisenfeld, Ferrara 1998; Dwek 1998; Hirashita 1999a, 1999b, 2000a; Edmunds 2001; Hirashita, et al. 2002a, 2002b; Hirashita, Ferrara 2002; Morgan, Edmunds 2003).

For several nearby spiral galaxies, there is a global linear correlation between the metallicity ( $Z$ ) and the dust-to-gas ratio ( $\mathcal{D}$ ) suggested by Issa, et al. (1990) observationally. This means that the dust-to-metal ratio is nearly constant for these spiral galaxies. A simple model developed by Hirashita (1999a) reproduces this global  $Z$ – $\mathcal{D}$  relation well. Edmunds (2001) argues that the dust-to-metal ratio does not change significantly during the entire galactic evolution based on his simple model. In short, the global  $Z$ – $\mathcal{D}$  relation can be interpreted as an evolutionary sequence by the model of Edmunds (2001): galaxies evolve from a point of lower  $Z$  and  $\mathcal{D}$  to another point of higher  $Z$  and  $\mathcal{D}$  with keeping a constant dust-to-metal ratio.

On the other hand, the  $Z$ – $\mathcal{D}$  relation for dwarf galaxies is not so tight; the dispersion reaches about an order of magnitude. Lisenfeld, Ferrara (1998) propose that outflows triggered by star-formation activity can cause such a large dispersion, whereas Hirashita et al. (2002b) show that the dispersion can result from a large variety of the efficiency of dust destruction by supernovae (SNe) shocks, even if there are no outflows; in their scenario the variety of the efficiency is caused by an intermittent star-formation history. In any case, the  $Z$ – $\mathcal{D}$  relation (or dust-to-metal ratio) is not universal, at least for dwarf galaxies.

What determines the dust-to-metal ratio? It is a very important question. Metal elements in the high- $z$  universe have already been detected (e.g., Pettini, et al. 1997). To

<sup>\*</sup> JSPS research fellow.

<sup>†</sup> Present address: Department of Physics, Kyoto University, Sakyo-ku, Kyoto 606-8502, akinoue@scphys.kyoto-u.ac.jp.

know the amount of dust (or extinction), we need to know what fraction of metals is condensed into dust. Recently, there are several models which can be used to calculate the spectral energy distribution of galaxies by solving the radiative transfer in the dusty ISM coupled with the chemical evolution model (e.g., Silva, et al. 1998; Takagi, et al. 2003). In these models, a dust-to-metal ratio, such as that in the Galaxy, is assumed. Is this really correct for dwarf galaxies, starburst galaxies, and high- $z$  galaxies?

In this paper, we investigate the evolution of the dust-to-metal ratio in galaxies by using a simple model for the evolution of the amount of dust and metal. Although Dwek (1998) presents the most detailed evolution model for the amount of metal and dust abundance for our Galaxy, we need not to trace so the detailed abundance of metal and the composition of dust. The aim of this paper is to discuss on a *global* (or *mean*) dust-to-metal ratio in a galaxy. Therefore, a simple treatment, as adopted in Hirashita's and Edmunds's work, is sufficient.

In the next section, we describe the model used in this paper. In the model, we take account of gas (and also metal) infall in order to discuss the time evolution on a real time-scale. Moreover, we reconsider the efficiency of the grain-growth process in the ISM. We then show in section 3 that the observed constancy of the dust-to-metal ratio in nearby spiral galaxies can be interpreted as a sequence of a similar galactic age. The achieved conclusions in this paper are summarized in the last section.

## 2. Model

Here, we describe the model used in this paper. First a set of equations and meanings of notations are summarized. We next explain the considered processes of dust formation, growth, and destruction in the ISM. Then, a set of parameters suitable for our Galaxy is estimated.

### 2.1. Equations

First of all, the basic assumptions adopted here are summarized as follows: (1) the ISM is treated as one zone, but two components. One is a cold dense cloud, and the other is a warm diffuse medium. The mass fraction of the cold cloud is fixed as a constant throughout the whole evolution of a galaxy. (2) Stars are formed only in the cold dense cloud following the Schmidt law of index 1. (3) The instantaneous recycling approximation is adopted. (4) Produced metal and dust are quickly mixed well in the ISM. (5) Dust consists of two components. One is the refractory core, and the other is the volatile mantle, which can exist only in a cold cloud. In other words, the mantle dust is destroyed quickly if it goes out of the cloud. (6) No outflow of the galactic scale.

Under the above assumptions, the time evolutions of the gas mass ( $M_{\text{gas}}$ ), the metal mass ( $M_Z$ ), the core dust mass ( $M_{\text{cor}}$ ), and the mantle dust mass ( $M_{\text{man}}$ ) are governed by the following equations:

$$\frac{dM_{\text{gas}}}{dt} = -(1 - R) \frac{\eta M_{\text{gas}}}{\tau_{\text{SF}}} + F, \quad (1)$$

**Table 1.** Notations and standard set.

Parameter	Value	Meaning
$\tau_{\text{SF}}$	5 Gyr	star formation time-scale
$\beta_{\text{in}}$	0.5	infall parameter ( $\equiv \tau_{\text{SF}}/\tau_{\text{in}}$ )
$R$	0.299	returned mass fraction
$y_Z$	0.025	stellar yield
$Z_{\text{in}}$	$0.01Z_{\odot}$	metallicity in infall gas
$f_c$	0.1	condensation efficiency
$\beta_{\text{SN}}$	10	SNe parameter ( $\equiv \tau_{\text{SF}}/\tau_{\text{SN}}$ )
$\tau_{\text{acc},0}$	$10^8$ yr	accretion growth time-scale
$\eta$	0.5	cold gas fraction
$\xi$	0.5	refractory probability

$$\frac{dM_Z}{dt} = -(1 - R) \frac{\eta M_Z}{\tau_{\text{SF}}} + y_Z \frac{\eta M_{\text{gas}}}{\tau_{\text{SF}}} + Z_{\text{in}}F, \quad (2)$$

$$\begin{aligned} \frac{dM_{\text{cor}}}{dt} = & -\frac{\eta M_{\text{cor}}}{\tau_{\text{SF}}} - \frac{M_{\text{cor}}}{\tau_{\text{SN}}} + f_c \left( R \frac{\eta M_Z}{\tau_{\text{SF}}} + y_Z \frac{\eta M_{\text{gas}}}{\tau_{\text{SF}}} \right) \\ & + \xi \frac{M_{\text{cor}}(1 - \delta_{\text{cl}})}{\tau_{\text{acc}}}, \end{aligned} \quad (3)$$

$$\frac{dM_{\text{man}}}{dt} = -\frac{M_{\text{man}}}{\tau_{\text{SF}}} + (1 - \xi) \frac{M_{\text{cor}}(1 - \delta_{\text{cl}})}{\tau_{\text{acc}}}, \quad (4)$$

where  $\tau_{\text{SF}}$ ,  $\tau_{\text{SN}}$ , and  $\tau_{\text{acc}}$  are the time scales of the star formation, dust destruction by SNe, and dust growth by metal accretion in the cold cloud, respectively. The term  $\eta M_{\text{gas}}/\tau_{\text{SF}}$  is the star-formation rate, where  $\eta$  is the mass fraction of the cold gas. The notations are summarized in table 1 and are described in the rest of this subsection. In section 3, we will solve equations (1)–(4) combined with the initial condition,  $M_{\text{gas}} = M_Z = M_{\text{cor}} = M_{\text{man}} = 0$  at  $t = 0$ .

We consider gas and metal infall from a halo, which can resolve the so-called G-dwarf problem of the stellar metallicity distribution in the Galaxy (e.g., Twarog 1980). Here, the gas infall rate is denoted by  $F$ , which is assumed to be the following analytic function:

$$F = \frac{M_0}{\tau_{\text{in}}} \exp[-t/\tau_{\text{in}}], \quad (5)$$

where  $\tau_{\text{in}}$  is the time-scale of infall and  $M_0$  is the total gas mass that can fall into the disk from the halo i.e.,  $\int F dt = M_0$ . The metallicity in the infalling gas is denoted as  $Z_{\text{in}}$ .

For the chemical evolution part [equations (1) and (2)], we need the returned mass fraction,  $R$ , and the stellar yield,  $y_Z$ . The returned fraction is the mass fraction of returned gas from stars into the ISM per unit mass of star formation, defined as

$$R = \int_{m_t}^{m_{\text{up}}} (m - w_m) \phi(m) dm, \quad (6)$$

where  $w_m$  is the remnant mass of a star with mass  $m$ ,  $m_t$  is the present turn-off mass, and  $\phi(m)$  is the initial mass function (IMF), normalized as

$$\int_{m_{\text{low}}}^{m_{\text{up}}} m \phi(m) dm = 1, \quad (7)$$

where  $m_{\text{low}}$  and  $m_{\text{up}}$  are the lower and upper cutoff masses of the IMF. When we assume the Salpeter IMF with  $m_{\text{low}} = 0.1M_{\odot}$ ,  $m_{\text{up}} = 100M_{\odot}$ , and  $m_{\text{t}} = 1M_{\odot}$ , and assume the remnant mass function in Pagel (1997), we obtain  $R = 0.299$ . The stellar yield is the mass fraction of the metal elements newly produced and ejected into the ISM per unit star formation, and defined as

$$y_Z = \int_{m_{\text{t}}}^{m_{\text{up}}} m p_Z(m) \phi(m) dm, \quad (8)$$

where  $p_Z(m)$  is the fractional mass of metal elements ejected into the ISM by a star of mass  $m$ . Assuming the Salpeter IMF with the same characteristic masses above and  $p_Z(m)$  in Pagel (1997), we obtain  $y_Z = 0.025$ .

In the part concerning the evolution of the amount of dust [equations (3) and (4)],  $f_c$  is the condensation efficiency in the stellar mass-loss gas, and  $\delta_{\text{cl}}$  is the dust-to-metal ratio in a cold cloud, i.e.,

$$\delta_{\text{cl}} = \frac{M_{\text{cor}}}{M_Z} + \frac{M_{\text{man}}}{\eta M_Z}. \quad (9)$$

Finally,  $\xi$  is the refractory probability of metal accretion. The refractory core may grow by an accretion process in the cold cloud as well as the volatile mantle. This parameter is defined as the fraction of accreted metal mass which contributes to the growth of the refractory core.

## 2.2. Grain Formation, Evolution, and Destruction

We first consider the condensation efficiency in the stellar outflow,  $f_c$ . The efficiency may depend on the stellar mass; different efficiencies between that in mass ejection by SNe and that in stellar wind from evolved stars are possible. In the framework presented here, we do not distinguish these two types of stellar mass-loss because of the instantaneous recycling approximation. Thus, the condensation efficiency given in this paper is an effective one, including both types of mass loss and averaged over the stellar mass by the assumed IMF. Moreover, the efficiency can evolve with the stellar metallicity. Indeed, Morgan, Edmunds (2003) suggest such an evolution, but the evolution is not very significant, fortunately. This is because the metal amounts in stellar outflows are often dominated by the newly produced metal. Therefore, we neglect the metallicity dependence of  $f_c$ , and assume a constant  $f_c$ .

The “stardust” injection rate is  $f_c(RZ + y_Z)\eta M_{\text{gas}}/\tau_{\text{SF}}$  [i.e., third term in equation (3)], where  $Z$  is the metallicity ( $= M_Z/M_{\text{gas}}$ ). On the other hand, the stellar mass-loss rate is  $R\eta M_{\text{gas}}/\tau_{\text{SF}}$ . Again, we note that the injection rate and the mass-loss rate include all types of stellar outflows. Thus, the dust-to-gas ratio in the mass-loss gas ( $\mathcal{D}_*$ ) is

$$\mathcal{D}_* = \frac{f_c(RZ + y_Z)}{R} \approx f_c \frac{y_Z}{R}. \quad (10)$$

The approximation in the last term is valid when  $Z \ll 4Z_{\odot}$  for  $R = 0.299$ ,  $y_Z = 0.025$ , and the solar metallicity  $Z_{\odot} = 0.02$ . Observationally,  $\mathcal{D}_* \sim 0.01$  is suggested as the present-day Galactic value (Gehrz 1989), although the uncertainty is still large. Therefore, we obtain  $f_c \sim 0.1$ ,

which agrees with values given by Hirashita (1999a, 1999b) and Edmunds (2001).

Next, we discuss the grain growth rate in the cold cloud. The dust mass increases if the metallic atoms accrete on the pre-existing grain cores. The refractory core, itself, may grow by accretion as well as the volatile mantle. If the accreted metal elements are refractory, such as Si, Fe, or Ti, the refractory core grows. On the other hand, elements such as C, N, and O produce a volatile mantle (maybe ice molecules) on the refractory core when these elements accrete onto the grain surface. Actually, the accretion rates of various elements are different from each other. To avoid such difficulty, we parameterize the situation by the refractory probability,  $\xi$ . This is defined as the mass fraction of accreted metal contributing to the growth of the refractory core.

The total (core+mantle) dust mass growth rate by metal accretion can be expressed as

$$\left[ \frac{dM_d}{dt} \right]_{\text{acc}} = N_{\text{cor}}^{\text{cl}} \pi a^2 s_Z \rho_Z^{\text{cl}} \langle v_Z \rangle, \quad (11)$$

where  $N_{\text{cor}}^{\text{cl}}$  is the number of refractory cores in the cold clouds,  $a$  is the typical grain radius,  $s_Z$  is the mean sticking coefficient of metal elements,  $\rho_Z^{\text{cl}}$  is the mass volume density of gaseous metallic atoms in the cold clouds, and  $\langle v_Z \rangle$  is the mean velocity of metallic atoms. We assumed a spherical grain for simplicity. Since  $N_{\text{cor}}^{\text{cl}} = \eta M_{\text{cor}}/m_d$  and  $\rho_Z^{\text{cl}} = \rho_{\text{gas}}^{\text{cl}} Z(1 - \delta_{\text{cl}})$ , where  $m_d$  is the typical grain mass and  $\rho_{\text{gas}}^{\text{cl}}$  is the volume mass density of the cold cloud gas, the dust mass growth rate is reduced to

$$\left[ \frac{dM_d}{dt} \right]_{\text{acc}} = \frac{M_{\text{cor}}(1 - \delta_{\text{cl}})}{\tau_{\text{acc}}}, \quad (12)$$

where we define the accretion time scale as  $\tau_{\text{acc}} = m_d/\eta \pi a^2 s_Z \rho_{\text{gas}}^{\text{cl}} \langle v_Z \rangle Z$ . We then obtain the fourth term in equation (3) and the second term in equation (4) by using the refractory probability,  $\xi$ . The parameter is determined later so as to reproduce the Galactic metallicity and dust-to-gas ratio.

The accretion time-scale,  $\tau_{\text{acc}}$ , is not constant during galaxy evolution, but depends on the metallicity. Here, we normalize it as

$$\tau_{\text{acc}} = \tau_{\text{acc},0}(Z_{\odot}/Z), \quad (13)$$

and we estimate the normalization,  $\tau_{\text{acc},0}$ , which means the accretion time-scale at the solar metallicity (i.e., the current value in the Galaxy). According to Hirashita (2000b), who estimated the grain growth time-scale by taking into account the mass function of the molecular clouds in the Galaxy,  $\tau_{\text{acc},0} \sim \eta^{-1} 5 \times 10^7$  yr. Although the cold gas fraction,  $\eta$ , is rather uncertain,  $\eta$  may not deviate significantly from 0.5. Thus, we always assume  $\tau_{\text{acc},0} \sim 10^8$  yr, except when indicated otherwise.

We next consider the dust-destruction rate. There are two processes for destruction; one is incorporation by star formation; the other is evaporation and sputtering in SNe remnants. Here, we assume that star formation occurs only in a cold cloud. Since the dust-to-gas ratio in a cold

cloud is  $(\eta M_{\text{cor}} + M_{\text{mantle}})/\eta M_{\text{gas}}$ , and the star-formation rate is  $\eta M_{\text{gas}}/\tau_{\text{SF}}$ , we obtain the first terms in equations (3) and (4) as the destruction rate by star formation of core and mantle, respectively. Here, we have assumed the destruction efficiency by star formation to be unity.

The SNe destroy only the core dust because the mantle dust is already destroyed in the SNe remnants, which are not cold gas. In fact, the SNe affect the amount of mantle dust through the cold gas fraction, which is reduced by the SNe. However, we assume a constant fraction of cold gas for simplicity. Since the dust-to-gas ratio in a warm medium is  $M_{\text{cor}}/M_{\text{gas}}$ , the destruction rate by SNe is

$$\left[ \frac{dM_d}{dt} \right]_{\text{SN}} = -\frac{M_{\text{cor}}}{M_{\text{gas}}} \epsilon M_{\text{SNR}} \gamma, \quad (14)$$

where  $\epsilon$  is the destruction efficiency,  $M_{\text{SNR}}$  is the gas mass shocked by one SN, and  $\gamma$  is the occurrence rate of SNe. We do not distinguish type Ia and type II SNe. Thus, the SNe-rate  $\gamma$  means the sum of the occurrence rates of both type Ia and type II. If we define the time-scale of the destruction by SNe as  $\tau_{\text{SN}} = M_{\text{gas}}/\epsilon M_{\text{SNR}} \gamma$  (McKee 1989), the second term in equation (3) is obtained.

Dwek (1998) proposed  $\tau_{\text{SN}}/\tau_{\text{acc},0} \simeq 2$  (constant). It was also assumed in Hirashita (1999a,b). Here, we reconsider this argument. When the star-formation rate is denoted as  $\psi (= \eta M_{\text{gas}}/\tau_{\text{SF}})$ , we find  $\tau_{\text{SN}}/\tau_{\text{SF}} = (\psi/\gamma)/(\eta \epsilon M_{\text{SNR}})$ . On the other hand, we have seen that  $\tau_{\text{acc},0} \propto \eta^{-1}$ . Thus, we find  $\tau_{\text{SN}}/\tau_{\text{acc},0} \propto (\psi/\gamma)\tau_{\text{SF}}$ . We may consider that the ratio of  $\psi$  and  $\gamma$  is roughly constant. Therefore, the ratio  $\tau_{\text{SN}}/\tau_{\text{acc},0}$  is proportional to  $\tau_{\text{SF}}$ . In other words, the ratio is not constant, as assumed by Dwek (1998), but dependent on the star-formation history (i.e.,  $\tau_{\text{SF}}$ ). This provides us with a new interpretation of the  $Z$ - $\mathcal{D}$  relation for nearby spiral galaxies presented in the next section. It is worth noting that we do not need the assumption of a constant  $\eta$  in the above statement.

Although the value of  $\eta$  is required when we estimate  $\tau_{\text{acc},0}$  and  $\tau_{\text{SF}}$ , estimating  $\eta$  is a rather complex task. After stars are formed and SNe occurs, the cold gas is heated by the SNe shocks, so that  $\eta$  decreases. When  $\eta$  decreases, the star-formation rate is suppressed, and then the SNe occurrence rate decreases, so that  $\eta$  increases. Thus, the star-formation rate ( $\propto \tau_{\text{SF}}^{-1}$ ) and  $\eta$  are coupled with each other non-linearly (Ikeuchi, Tomita 1983; Hirashita 2000a). To avoid the complex task of solving a set of non-linear equations to determine  $\eta$ , we assume a constant  $\eta$  as an average value during the galaxy evolution time-scale for simplicity. For a constant  $\eta$ , the ratio of  $\tau_{\text{SN}}$  to  $\tau_{\text{SF}}$  becomes a constant. Since McKee (1989) estimates  $\tau_{\text{SN}} \simeq 4 \times 10^8$  yr for the Galaxy and  $\tau_{\text{SF}} \sim 5 \times 10^9$  yr is suitable for the Galaxy, we obtain  $\tau_{\text{SF}}/\tau_{\text{SN}} \sim 10$ . Combining  $\tau_{\text{acc},0} \sim 10^8$  yr, we find

$$\frac{\tau_{\text{SN}}}{\tau_{\text{acc},0}} \sim \left( \frac{\tau_{\text{SF}}}{1 \text{ Gyr}} \right). \quad (15)$$

In future work, the fraction  $\eta$  should be determined self-consistently in the model.

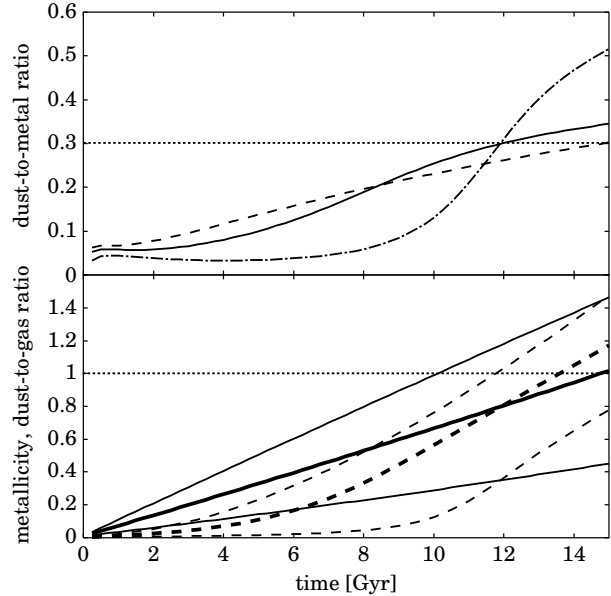


**Fig. 1.** Time evolution of the metallicity, dust-to-gas ratio, and dust-to-metal ratio. *Bottom* : the solid curves indicate the metallicity and the dashed curves indicate the dust-to-gas ratio. The vertical axis is normalized by the present-day Galactic value, which is indicated by the dotted straight line. The thick curves are the standard case (table 1), the top thin (solid and dashed) curves are the case of  $\eta = 0.8$  and  $\xi = 0$ , and the bottom thin curves are the case of  $\eta = 0.2$  and  $\xi = 1$ , where  $\eta$  is the cold gas fraction and  $\xi$  is the refractory probability in the accretion process. *Top* : the solid, dashed, and dash-dotted curves are the standard case,  $\eta = 0.8$  and  $\xi = 0$  case, and  $\eta = 0.2$  and  $\xi = 1$  case, respectively. The dotted straight line indicates the present-day Galactic value.

### 2.3. Standard Case (Milky Way)

Here, we estimate a set of parameters suitable for our Galaxy. First, the time-scales of the star formation and infall are discussed. Takeuchi, Hirashita (2000) have examined the star-formation history of the Galaxy by using a chemical evolution model with infall similar to that used in this paper. According to them, a set of these time-scales between  $(\tau_{\text{SF}}, \tau_{\text{in}}) = (6, 23)$  and  $(11, 12)$  in Gyr unit can reproduce the observed star-formation history of the galactic disk, the age–metallicity relation of stars in the solar neighborhood, and the metallicity distribution of G-dwarfs. Noting that their star-formation rate and that in this paper are different in the treatment of the cold-gas fraction ( $\eta$ ), we adopt  $\tau_{\text{SF}} = 5$  Gyr and  $\tau_{\text{in}} = 10$  Gyr. Combining these time-scales with  $R = 0.299$  and  $yz = 0.025$  (see subsection 2.1), and assuming a very low metallicity in the infall gas (for example  $Z_{\text{in}} = 0.01 Z_{\odot}$ ), we find that the present-day (age  $\sim 12$  Gyr) metallicity becomes around Solar metallicity (see figure 1 bottom panel), which ensures the validity of these time-scales.

For the convenience of later discussions, we define the infall parameter,  $\beta_{\text{in}}$ , as  $\tau_{\text{SF}}/\tau_{\text{in}}$ . Thus, we adopt  $\beta_{\text{in}} = 0.5$  for our Galaxy. Since an infall parameter suitable for other galaxies with a different star-formation history (i.e.,  $\tau_{\text{SF}}$ ) is rather unknown, we assume  $\beta_{\text{in}} = 0.5$  for all

galaxies. The effect of the other choices of  $\beta_{\text{in}}$  is discussed in subsection 3.2.

We use values estimated in subsection 2.2 for parameters  $f_c$ ,  $\beta_{\text{SN}} \equiv \tau_{\text{SF}}/\tau_{\text{SN}}$ , and  $\tau_{\text{acc},0}$ . Strictly speaking,  $\tau_{\text{acc},0}$  depends on  $\eta$ , as shown in subsection 2.2. Nevertheless, we adopt a constant  $\tau_{\text{acc},0} = 10^8$  yr for simplicity because the uncertainty of  $\tau_{\text{acc},0}$  is large and  $\eta$  may be roughly  $\sim 0.5$ .

We now modulate two parameters of  $\eta$  (cold gas fraction) and  $\xi$  (refractory probability in accretion) so as to reproduce the present-day dust-to-metal ratio in the Galaxy. Adopting the solar metallicity (0.02) and the dust-to-gas ratio in the solar neighborhood ( $6 \times 10^{-3}$ ; Spitzer 1978) as the present-day  $Z$  and  $\mathcal{D}$  in the Galaxy, we find the present-day dust-to-metal ratio,  $\delta = (M_{\text{cor}} + M_{\text{man}})/M_{\text{gas}} = 0.3$ . In figure 1, we show the time evolution of the metallicity, the dust-to-gas ratio, and the dust-to-metal ratio for three sets of  $\eta$  and  $\xi$ : (1)  $\eta = \xi = 0.5$ , (2)  $\eta = 0.8$  and  $\xi = 0$ , and (3)  $\eta = 0.2$  and  $\xi = 1$ . All of these cases give the calculated  $\delta \simeq 0.3$  at the galactic age of 12–15 Gyr (top panel in figure 1). From the bottom panel of figure 1, we find that the case of  $\eta = \xi = 0.5$  is the best. Thus, we call this case the 'standard case', whose parameters are summarized in table 1.

Although the case of  $\eta = 0.2$  and  $\xi = 1$  is not suitable for the Galaxy, because of the too small metallicity, the case of  $\eta = 0.8$  and  $\xi = 0$  is not so bad. Since the time evolution of the dust-to-metal ratio in this case is very similar to that of the standard case, our results obtained later are not altered if we choose this case as the standard case. We note here that the parameter set given in table 1, as the standard set, is not a unique solution for the Galaxy. There may be other sets which can reproduce all observational constraints for the Galaxy. However, we do not have enough data for determining a unique solution, even for the Galaxy. For example, we can determine  $\xi$  if we know the mass ratio of the grain core and mantle, which is still unknown. In future work, we may determine these parameters more precisely.

It is important that the dust-to-metal ratio in young galaxies can be much smaller than that in the present-day Galaxy, as shown in the top panel of figure 1. Therefore, a galaxy does not evolve with a constant dust-to-metal ratio. That is, we cannot consider the  $Z$ – $\mathcal{D}$  relation of Issa et al. (1990) to be an evolutionary sequence, like Edmunds (2001). We discuss what the  $Z$ – $\mathcal{D}$  relation implies in the next section.

### 3. Results and Discussions

#### 3.1. $Z$ – $\mathcal{D}$ Relation

Here, we compare the observed  $Z$ – $\mathcal{D}$  relation with our theoretical ones. First, the observational data used are explained. Although a large and systematic data set of  $Z$  and  $\mathcal{D}$  of various types of galaxies is required, we cannot find such a data set. Thus, we use the data presented by Issa et al. (1990), whose sample galaxies are five nearby spiral galaxies (the Galaxy, M 31, M 33, M 51, and M 101) and both Magellanic clouds. Lisenfeld, Ferrara (1998)

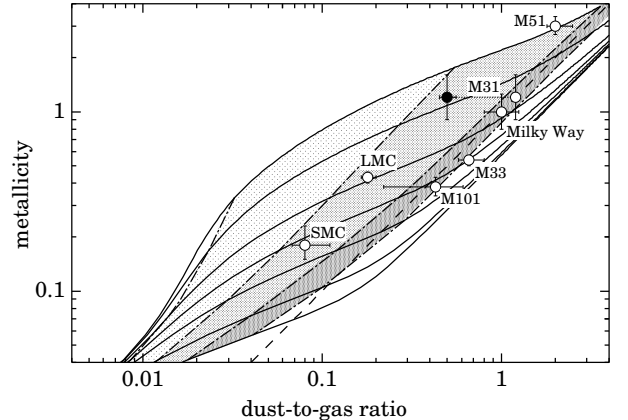


**Fig. 2.** Metallicity ( $Z$ )–dust-to-gas ratio ( $\mathcal{D}$ ) relation. The vertical and horizontal axes are normalized by  $Z_{\odot}$  and  $\mathcal{D}$  of the Galaxy, respectively. The open circles are observed data of  $Z$  and  $\mathcal{D}$  for five nearby spiral galaxies and Magellanic clouds taken from Issa et al. (1990), except for M 31 whose  $\mathcal{D}$  is taken from Inoue (2001). The filled circle is M 31 taken from Issa et al. (1990). The solid curves are theoretical  $Z$ – $\mathcal{D}$  relations; the adopted star formation time-scale  $\tau_{\text{SF}} = 1, 2, 5, 10, 20, 50$ , and 100 Gyr from top to bottom. Other parameters are the same as those in table 1. The dash-dotted curves indicate the iso-galactic age; 1, 5, 10, and 15 Gyr from left to right. That is, the thin, medium, and thick shaded areas indicate that the galactic age is in 1–5 Gyr, 5–10 Gyr, and 10–15 Gyr, respectively. The dashed straight line represents the sequence of the same dust-to-metal ratio as the Galaxy.

and Hirashita et al. (2002b) compiled such data of dwarf galaxies. However, since their  $\mathcal{D}$ s of dwarf galaxies are based only on IRAS data, there may be systematic underestimations due to the cold dust not detected by IRAS (e.g., Popescu, et al. 2002). Thus, we decided to use only Issa's data. For M 31, the dust-to-gas ratio estimated in Inoue (2001) from the data obtained by ISO was also used. It is very useful to examine the  $Z$ – $\mathcal{D}$  relation for a large sample of galaxies in future work.

In figure 2, we display a comparison between the observed data points and the theoretical predictions with various star-formation histories (i.e.,  $\tau_{\text{SF}}$ ). The adopted  $\tau_{\text{SF}}$ s are 1, 2, 5, 10, 20, 50, and 100 Gyr from top to bottom. They are suitable for early- to late-type galaxies from top to bottom. In our model, a different evolutionary path in the  $Z$ – $\mathcal{D}$  plane is predicted depending on  $\tau_{\text{SF}}$ . This is because  $\tau_{\text{SN}}/\tau_{\text{acc},0}$  is not constant, but dependent on  $\tau_{\text{SF}}$ , as discussed in subsection 2.2 [equation (15)]. In other words, the accretion time-scale does not depend on  $\tau_{\text{SF}}$ , whereas the SNe destruction time-scale depends on it. The separation of these evolutionary sequences is caused by the different efficiency of the dust destruction by SNe relative to the accretion growth of dust. A more rapid star formation causes a higher occurrence rate of SNe, and results in a more efficient destruction of dust.

How can we understand the observed constancy of the dust-to-metal ratio in nearby spiral galaxies within the framework of our model? The answer is that the sequence of the dust-to-metal ratio is the sequence of a constant galactic age. As shown in figure 2, these spiral galaxies

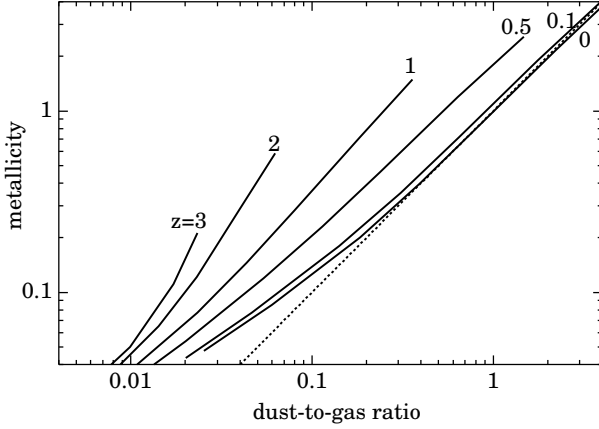


**Fig. 3.** Predicted redshift evolution of  $Z$ - $D$  relation. The solid curves are the predicted  $Z$ - $D$  relation at  $z = 3, 2, 1, 0.5$ , and 0 (local) from left to right, as indicated in the panel. The dotted straight line represents the sequence of the same dust-to-metal ratio as the Galaxy. The vertical and horizontal axes are the same mean as those of figure 2. The present-day galactic age is assumed to be 12 Gyr. The adopted cosmology is  $\Omega_M = 0.3$ ,  $\Omega_\Lambda = 0.7$ , and  $H_0 = 70 \text{ km s}^{-1} \text{ Mpc}^{-1}$ . The vertical and horizontal axes are normalized by  $Z_\odot$  and  $D$  of the Galaxy, respectively.

are plotted in (or around) the area with an age of 10–15 Gyr (thick shaded area). Therefore, we conclude that the observed linear  $Z$ - $D$  relation for the nearby spiral galaxies is not an evolutionary sequence with a constant dust-to-metal ratio, but a sequence of a similar galactic age with various star-formation histories (i.e., from early- to late-type). This is the main conclusion of this paper.

As shown in figure 1, our model predicts a time evolution of the dust-to-metal ratio: a lower dust-to-metal ratio in younger galaxies. Thus, the  $Z$ - $D$  relation is expected to evolve with the galactic age or redshift. We show such redshift evolution of the  $Z$ - $D$  relation in figure 3, where we assume the galactic age at the present-day to be 12 Gyr. We predict a deviation from the local  $Z$ - $D$  relation at  $z > 0.5$ . Therefore, the investigation of the  $Z$ - $D$  relation in a high- $z$  will be a good test against our model. Observations with, for example, ASTRO-F and SIRTF will be very useful.

Finally, we comment on the Magellanic clouds. They are plotted in a somewhat younger area in figure 2 than other spiral galaxies. They are found in the area of an age of 5–10 Gyr (medium shaded area). The definition of the galactic age in the model is the time from the start of the main gas infall and star formation because our treatment is one-zone. If a minor star formation exists before the main one, we underestimate the galactic age. Thus, the younger ages of Magellanic clouds may be due to such an effect.

### 3.2. Effect of SNe, Accretion, and Infall Time-Scales

In this subsection we discuss the effect on our interpretation of the local  $Z$ - $D$  relation when we change  $\tau_{\text{SN}}$ ,  $\tau_{\text{acc},0}$ , and  $\tau_{\text{in}}$ . Edmunds (2001) argues that the accretion time scale is much shorter than that adopted here,

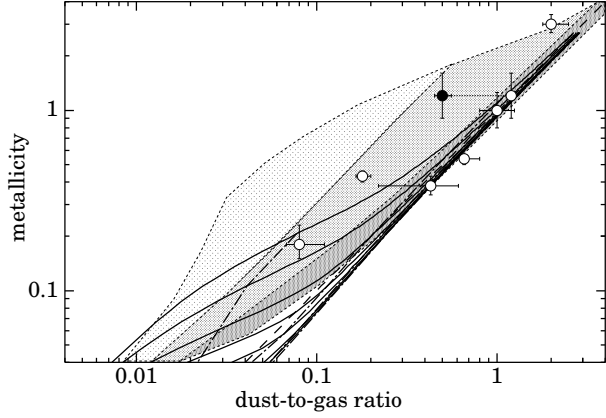


**Fig. 4.** Same as figure 2, but  $\tau_{\text{acc},0} = 10^7 \text{ yr}$  and  $\eta = 0.3$  are adopted. The thin, medium, and thick shaded areas indicate the same areas as in figure 2 for a comparison. The vertical and horizontal axes are normalized by  $Z_\odot$  and  $D$  of the Galaxy, respectively.

and that the dust destruction by SNe is not efficient. Indeed, he assumes the sticking probability on the grain surface in the accretion process of the metallic atoms to be unity, whereas our estimate is based on the value of Hirashita (2000b), who assumes a sticking probability of 0.1. The accretion time scale becomes an order of magnitude shorter than that in table 1 if we assume a sticking probability of unity.

In figure 4, the high accretion cases are displayed. All curves and points, except for the shaded areas, have the same meanings as in figure 2, but  $\tau_{\text{acc},0} = 10^7 \text{ yr}$  and  $\eta = 0.3$  are adopted. The value of  $\eta$  is determined so as to reproduce the parameters of the Galaxy, as done in subsection 2.3. The shaded areas cover the same areas as figure 2 for a comparison. We find that the variation of the  $Z$ - $D$  relations becomes small and the evolutionary tracks of various  $\tau_{\text{SF}}$  are almost superposed on the dashed straight line, which is a sequence of the same dust-to-metal ratio as the Galaxy if the galactic age is larger than about 5 Gyr. This means that the local  $Z$ - $D$  relation of spiral galaxies can be interpreted as the evolutionary sequence. Of course, we can interpret it as a sequence of similar galactic age, although sequences of age larger than about 5 Gyr cannot be distinguished from each other.

In figure 5, we display the case of no SNe destruction. All curves and points, except for the shaded areas, have the same meanings as in figure 2, but  $\beta_{\text{SN}} = 0$ ,  $\eta = 0.3$ , and  $\xi = 0$  are adopted. The values of  $\eta$  and  $\xi$  are adjusted so as to reproduce the Galactic parameters. The shaded areas indicate the same areas as in figure 2 for a comparison. We find a similar trend to the high accretion case, a tighter  $Z$ - $D$  relation. We can again interpret the local  $Z$ - $D$  relation as the evolutionary sequence.

Although the data point of the Large Magellanic Cloud cannot be covered by the no SNe destruction and high accretion unless  $\tau_{\text{SF}} < 1$  Gyr, this may not be so critical because the uncertainty of the data point is likely to be larger than its error-bars shown in figures 2, 4, and 5.

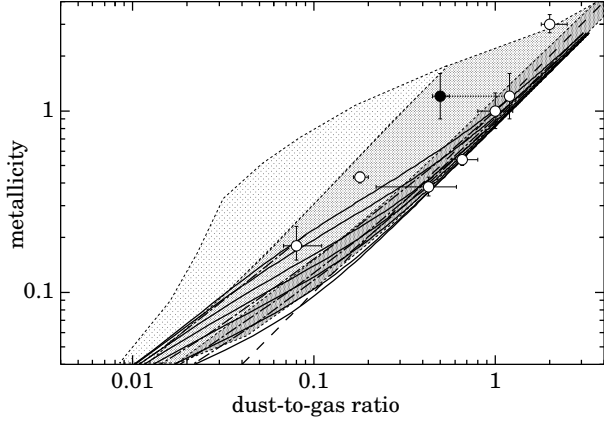


**Fig. 5.** Same as figure 2, but  $\beta_{\text{SN}} = \tau_{\text{SF}}/\tau_{\text{SN}} = 0$ ,  $\eta = 0.3$ , and  $\xi = 0$  are adopted. The thin, medium, and thick shaded areas indicate the same areas as in figure 2 for a comparison. The vertical and horizontal axes are normalized by  $Z_{\odot}$  and  $\mathcal{D}$  of the Galaxy, respectively.

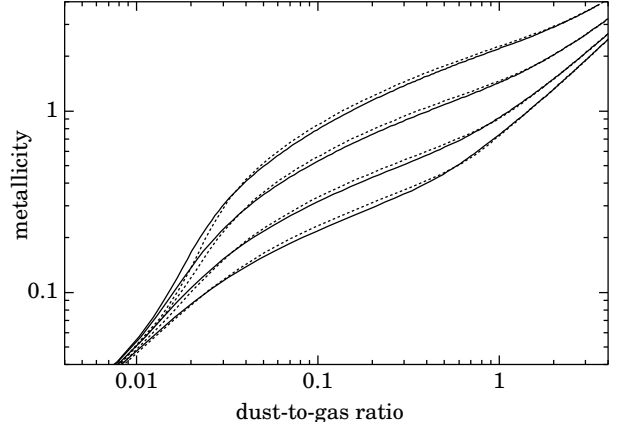


**Fig. 7.** Effect of infall on the  $Z$ - $\mathcal{D}$  relation. The solid and dotted curves are the  $\beta_{\text{in}} = 0.5$  and no infall cases, respectively. The adopted  $\tau_{\text{SF}} = 1, 2, 5$ , and 10 Gyr from top to bottom. The vertical and horizontal axes are normalized by  $Z_{\odot}$  and  $\mathcal{D}$  of the Galaxy, respectively.

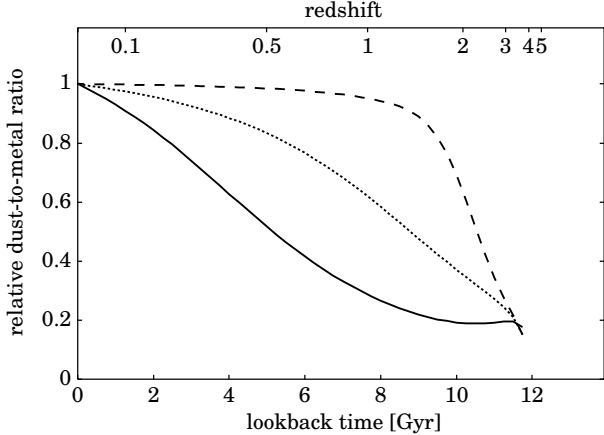


**Fig. 6.** Time evolution of the dust-to-metal ratio. The vertical axis is normalized by the present-day value. The solid, dotted, and dashed curves are the standard (table 1), no SNe destruction, and high accretion cases, respectively. For all curves,  $\tau_{\text{SF}} = 5$  Gyr and the present-day galactic age of 12 Gyr are assumed. The adopted cosmology is  $\Omega_M = 0.3$ ,  $\Omega_{\Lambda} = 0.7$ , and  $H_0 = 70 \text{ km s}^{-1} \text{ Mpc}^{-1}$ .

Therefore, we cannot distinguish the standard, no SNe destruction, and the high-accretion cases only by the local  $Z$ - $\mathcal{D}$  relation. However, fortunately, these three cases can be distinguished if we have information about the  $Z$ - $\mathcal{D}$  relation of younger galaxies.

In figure 6, we show the dust-to-metal ratios of the standard, no SNe destruction, and high accretion as a function of the lookback time and redshift. A present-day galactic age of 12 Gyr and  $\tau_{\text{SF}} = 5$  Gyr are assumed. From this figure, we find that the dust-to-metal ratios of the standard and no SNe destruction cases at  $z = 1$  become 30% and 60% of the local value, respectively, whereas that of the high-accretion case does not change significantly. Thus, we can obtain further constraints on  $\tau_{\text{SN}}$  and  $\tau_{\text{acc},0}$  by using observations of the  $Z$ - $\mathcal{D}$  relation at  $z \sim 1$  (or local

galaxies with an age of several Gyr).

The effect of infall on the  $Z$ - $\mathcal{D}$  relation is discussed. In Figure 7, we show the comparison between the standard cases and the no infall cases. Clearly we find the effect of infall is negligible in the plane of  $Z$  and  $\mathcal{D}$ . However, the infall parameter  $\beta_{\text{in}}$  affects the speed of the chemical enrichment. Thus, a galaxy without infall rapidly evolves in the  $Z$ - $\mathcal{D}$  plane along the track determined from the combination of parameters,  $\tau_{\text{acc},0}$ ,  $\beta_{\text{SN}}$ ,  $\eta$ , and  $\xi$ . Therefore, the dispersion of  $\beta_{\text{in}}$  can disturb the  $Z$ - $\mathcal{D}$  relation of a constant galactic age as shown in Figure 3.

### 3.3. Implication for Very Young Galaxies

All our models considered in figure 6 predict that the dust-to-metal ratio in a galaxy younger than about 1 Gyr is very small, about one-fifth of the present-day Galactic value (dust/metal  $\lesssim 0.1$ ). Because of the instantaneous recycling approximation, the accuracy of the model result may not be so good for such very young galaxies. Nevertheless, we discuss what our model implies against very young galaxies whose age is less than 1 Gyr.

First, we compare our model prediction with observations of a nearby dwarf galaxy, SBS 0335–052. This dwarf galaxy has an age of less than about 100 Myr (Izotov, et al. 1997). In figures 8 and 9, we show such comparisons. The allowed range of the metallicity is taken from Izotov, et al. (1997). That of the dust-to-gas ratio is based on the infrared spectral energy distribution (Dale, et al. 2001) and the hydrogen Brackett lines ratio (Hunt, et al. 2001). For theoretical predictions, we assume  $\tau_{\text{SF}} = 1$  (thick curves) and 5 (thin curves) Gyr. As can be seen in figure 8, the effect of the metallicity in the infalling gas, which is assumed to be  $0.01Z_{\odot}$ , appears in the solid ( $\eta = 0.5$ ) and dashed ( $\eta = 0.3$ ) curves. The dash-dotted and dotted curves are the cases of zero metal infall and no infall, respectively. From these figures, we find that our model reproduces the observed metallicity, dust-to-gas ratio, and very young age quite well if we assume  $\tau_{\text{SF}} = 1$

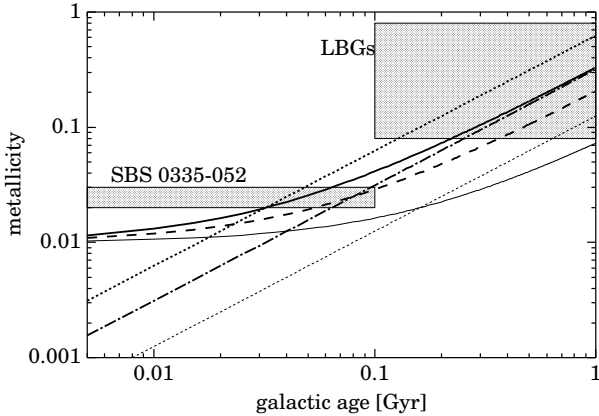


**Fig. 8.** Metallicity evolution at a galactic age of less than 1 Gyr. The solid curves are the standard case. The dashed, dotted, and dash-dotted curves are the cases of  $\eta = 0.3$ , no infall, and  $Z_{\text{in}} = 0$ , respectively. The assumed  $\tau_{\text{SF}} = 1$  Gyr and 5 Gyr for the thick and thin curves, respectively. The shaded areas are the areas indicated from observations of a nearby dwarf galaxy, SBS 0335–052, and the Lyman break galaxies at  $z \sim 3$ , as denoted in the panel. The vertical axis is normalized by  $Z_{\odot}$ .

Gyr. Such a short time-scale of the star formation, i.e., a starburst like time-scale, is reasonable for SBS 0335–052 because the galaxy is really starbursting now.

Next, we move on a comparison with the Lyman break galaxies (LBGs) at  $z \sim 3$ . The LBGs seem to have an age from about 100 Myr to 1 Gyr (e.g., Shapley, et al. 2001) and a metallicity around one-third of the Solar value (e.g., Pettini, et al. 2001). The dust-to-gas ratio in the LBGs is still quite uncertain. We compare only the metallicity of the LBGs with our model. figure 8 shows that our models with  $\tau_{\text{SF}} = 1$  Gyr reproduce the observed metallicity and age of the LBGs very well. In figure 9, we present the expected range of the dust-to-gas ratio in the LBGs (the thin shaded area); 0.01–0.1 of the dust-to-gas ratio of our Galaxy. Our model predicts that the dust-to-metal ratio in the LBGs is  $\sim 0.1$  or less. This prediction should be tested in the future.

For very young galaxies, our model predicts a lower dust-to-metal ratio than that in Edmunds (2001) and Morgan, Edmunds (2003). This is caused by the different assumptions between both models, for example, a low or high accretion efficiency (sticking coefficient), effective or no SNe destruction, with or without galactic gas infall. However, our smaller dust-to-metal ratio does not predict more transparent young galaxies straightforwardly. This is because the amount of attenuation depends on the dust optical depth, which is strongly affected by the geometry of the dust distribution. If the dust grains are confined in a small area, a large attenuation is expected, even in a small dust amount. Of course, the clumpiness of the distribution is also important.

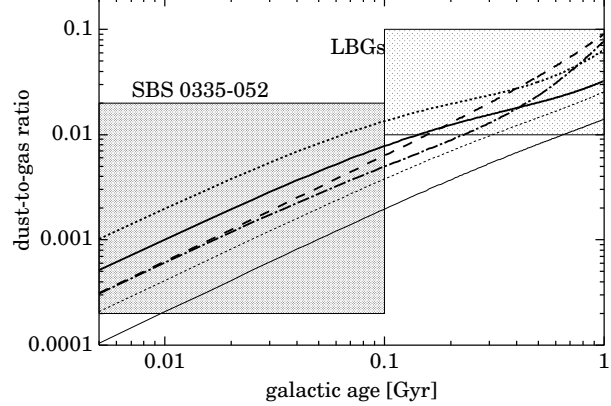


**Fig. 9.** Dust-to-gas ratio evolution at a galactic age of less than 1 Gyr. The thick solid, dashed, dash-dotted, and dotted curves are the cases of the standard, no SNe destruction, high accretion growth, and no infall with  $\tau_{\text{SF}} = 1$  Gyr, respectively. The thin solid and dotted curves are the standard and no infall with  $\tau_{\text{SF}} = 5$  Gyr, respectively. The effect of metallicity in the infalling gas is negligible in this plot. The thick shaded area is the area indicated from the observations of SBS 0335–052. The thin shaded area is the expected area of the Lyman break galaxies at  $z \sim 3$ . The vertical axis is normalized by the dust-to-gas ratio of our Galaxy.

#### 4. Conclusion

We construct a simple evolutionary model of the amount of metal and dust in order to discuss the evolution of the dust-to-metal ratio in galaxies. Then, the achieved conclusions are summarized as follows:

(1) We propose that the grain growth time-scale by the metal accretion normalized by the gas metallicity ( $\tau_{\text{acc},0}$ ) does not depend on the star-formation history ( $\tau_{\text{SF}}$ ) significantly. If this is correct, the ratio of the time-scale of dust destruction by SNe ( $\tau_{\text{SN}}$ ) to that of the accretion growth depends on the star-formation history because only  $\tau_{\text{SN}}$  depends on  $\tau_{\text{SF}}$ . On the contrary, a constant ratio  $\tau_{\text{SN}}/\tau_{\text{acc},0}$  has been assumed in previous studies, such as Dwek (1998).

(2) The evolutionary track in the plane of the metallicity ( $Z$ ) and the dust-to-gas ratio ( $\mathcal{D}$ ) depend on the ratio  $\tau_{\text{SN}}/\tau_{\text{acc},0}$ , or equivalently on the star-formation history,  $\tau_{\text{SF}}$ .

(3) The observed linearity of the  $Z$ – $\mathcal{D}$  relation for nearby spiral galaxies is interpreted as the sequence of a constant galactic age in our framework.

(4) The dust-to-metal ratio can evolve significantly during the evolutionary time-scale of galaxies: the ratio may be 50%, 30% and 20% of the local value at  $z \sim 0.5$ , 1, and  $\gtrsim 2$ , respectively. Therefore, we will observe  $Z$ – $\mathcal{D}$  relations different from the local one for high- $z$  (or young) galaxies.

(5) The uncertainties concerning the time-scales of dust destruction by SNe and dust growth by accretion are still large, and different parameter choices result in different evolutions of the dust-to-metal ratio. Fortunately, we can put a further constraint on these time-scales by using

the observations of the dust-to-metal ratio in high- $z$  (or young) galaxies. Therefore, such observations are strongly encouraged.

(6) The effect of infall on evolutionary tracks in the  $Z$ – $D$  plane is negligible. However, since the speed of chemical enrichment depends on the infall rate, the dispersion of the infall rate can disturb the  $Z$ – $D$  relation of a constant galactic age.

(7) Our model shows a very good agreement with the observations of a nearby extremely young (age  $\lesssim 100$  Myr) dwarf galaxy, SBS 0335–052. We suggest that the Lyman break galaxies at  $z \sim 3$  have a low dust-to-metal ratio of 0.1, or less. Although our model predicts a relatively smaller amount of dust in high- $z$  galaxies, it does not mean the transparent high- $z$  galaxies, because the dust opacity strongly depends on the geometry of the dust distribution.

The author thanks the referee, Dr. M. G. Edmunds, for his great efforts to understand this work, and also thank Ryuko Hirata and Hideyuki Kamaya for continuous encouragement. This work is financially supported by the Research Fellowships of the Japan Society for the Promotion of Science for Young Scientists.

## References

Audouze, J., & Tinsley, B. T. 1976, ARA&A, 14, 43

Buat, V., Boselli, A., Gavazzi, G., & Bonfanti, C. 2002, A&A, 383, 801

Dale, D. A., Helou, G., Neugebauer, G., Soifer, B. T., Frayer, D. T., & Condon, J. J. 2001, AJ, 122, 1736

Dwek, E. 1998, ApJ, 501, 643

Dwek, E., & Scalo, J. M. 1980, ApJ, 239, 193

Edmunds, M. G. 2001, MNRAS, 328, 223

Gehrz, R. D. 1989, in IAU Symp. 135, Interstellar Dust, ed. L. J. Allamandola & A. G. G. M. Tielens (Dordrecht: Kluwer), 445

Hirashita, H. 1999a, ApJ, 510, L99

Hirashita, H. 1999b, ApJ, 522, 220

Hirashita, H. 2000a, ApJ, 531, 693

Hirashita, H. 2000b, PASJ, 52, 585

Hirashita, H., & Ferrara, A. 2002, MNRAS, 337, 921

Hirashita, H., Hunt, L. K., & Ferrara, A. 2002a, MNRAS, 330, L19

Hirashita, H., Tajiri, Y. Y., & Kamaya, H. 2002b, A&A, 388, 439

Hunt, L. K., Vanzi, L., & Thuan, T. X. 2001, A&A, 377, 66

Ikeuchi, S., & Tomita, H. 1983, PASJ, 35, 77

Inoue, A. K. 2001, AJ, 122, 1788

Issa, M. R., MacLaren, I., & Wolfendale, A. W. 1990, A&A, 236, 237

Izotov, Y. I., Lipovetsky, V. A., Chaffee, F. H., Foltz, C. B., Guseva, N. G., & Kniazev, A. Y. 1997, ApJ, 476, 698

Lisenfeld, U., & Ferrara, A. 1998, ApJ, 496, 145

McKee, C. F. 1989, in IAU Symp. 135, Interstellar Dust, ed. L. J. Allamandola & A. G. G. M. Tielens (Dordrecht: Kluwer), 431

Morgan, H. L., & Edmunds, M. G. 2003, MNRAS, 343, 427

Pagel, B. E. J. 1997, Nucleosynthesis and Chemical Evolution of Galaxies (Cambridge: Cambridge Univ. Press), 209

Pettini, M., Shapley, A. E., Steidel, C. C., Cuby, J.-G., Dickinson, M., Moorwood, A. F. M., Adelberger, K. L., & Giavalisco, M. 2001, ApJ, 554, 981

Pettini, M., Smith, L. J., King, D. L., & Hunstead, R. W. 1997, ApJ, 486, 665

Popescu, C. C., Tuffs, R. J., Völk, H. J., Pierini, D., & Madore, B. F. 2002, ApJ, 567, 221

Shapley, A. E., Steidel, C. C., Adelberger, K. L., Dickinson, M., Giavalisco, M., & Pettini, M. 2001, ApJ, 562, 95

Silva, L., Granato, G. L., Bressan, A., & Danese, L. 1998, ApJ, 509, 103

Spitzer, L., Jr. 1978, Physical Processes in the Interstellar Medium (New York: Wiley), 162

Takagi, T., Arimoto, N., & Hanami, H. 2003, MNRAS, 340, 813

Takeuchi, T. T., & Hirashita, H. 2000, ApJ, 540, 217

Tinsley, B. M. 1980, Fundam. Cosmic Phys., 5, 287

Twarog, B. A. 1980, ApJ, 242, 242

Wang, B. 1991, ApJ, 374, 456

Whittet, D. C. B. 2003, Dust in the Galactic Environment, 2nd ed. (Bristol: Institute of Physics), 24